

GT2011-46513

MAGNETIC-AEROSTATIC HYBRID BEARING FOR MINI-TYPE HIGH-SPEED AIR TURBINE CARTRIDGE

Shih-Chun Wang Kuang-Yuh Huang

Department of Mechanical Engineering

National Taiwan University

10716 Taipei, Taiwan

E-mail: f91522612@ntu.edu.tw, kyhuang@ntu.edu.tw

ABSTRACT

Under the development trend of high speed and high efficiency, mini-type air turbines have been widely applied to high-speed dental handpieces for decades. Bearing is the key component deciding efficiency of mini-type air turbine. Friction, collision and wear are the main causes to let the traditional ball and roller bearing not be able to reach higher efficiency. Although aerostatic bearing can realize very small sliding friction, but its weak bearing characteristic limits its application. In our research, we combined a magnetic levitation bearing with an aerostatic bearing to create a novel magnetic-aerostatic hybrid bearing, which can significantly promote the mini-type air turbine in a dental handpiece to achieve a better high-speed performance. The aerostatic bearing undertakes the function of radial bearing, and the magnetic levitation is responsible for the thrust bearing. The aerostatic bearing utilizes a composite orifice form with a large depth to width aspect ratio that can be realized by simple machining process. Its radial arranged orifices provide the spindle a sufficient and uniform radial support with high pressured air film. In consideration of operational safety and size constraint of the dental handpiece, the passive magnetic levitation method with repulsive NdFeB magnet rings is adopted for the thrust bearing. For comprehending their characteristics of the aerostatic and the magnetic levitation bearings, the finite element analytical method is employed to investigate the relationship between system parameters and performance and also to deduce the optimal construction for the prototype development. Our developed magnetic-aerostatic hybrid bearing is also experimentally approved to be able to provide stable and sustainable bearing capacity under low air pressure condition.

Keywords: Air turbine cartridge, Hybrid bearing, Aerostatic bearing, Magnetic levitation bearing, Radial bearing, Thrust bearing, High bearing capacity, High speed

1. INTRODUCTION

Mini-type air turbines with speed above 400,000 rpm, as our research subject in this paper, have been applied in the precision machinery industry, such as micro drilling machine, dental handpiece, and micro-turbine engine, etc... For realizing efficient and precision machining, air turbine must provide more stable and high speed for driving more miniaturized tool to create enough cutting speed. However, in order to efficiently enhance their speed and durability and to decrease noise and vibration in high-speed operation, traditional contact bearing must be replaced by non-contact bearing.

The relatively expensive high-speed mini-type air turbine cartridge usually adopts an aerostatic bearing group, which possesses axial and the radial bearing capacities. With bearing force from the high-pressure air mainly adopted by the aerostatic bearing, the spindle can float over the stator only through an air gap without any contact. Due to its very low viscosity, the air gap only deduces minimal frictional force to the rotating spindle. Therefore, compared with traditional contact bearing, the aerostatic bearing can significantly reduce frictional loss to efficiently enhance energy utilization. Besides, various thermal influences induced by frictional loss can be also effectively kept under control. In addition, the self-homogenization effect of the pressured air can also compensate for some machining errors on the bearing surface, thus well increasing the rotational accuracy of the spindle.

For achieving non-contact operation, the well-known bearing forms include fluid, air, magnetic and electrostatic bearings. Because of the crucial requirements -size constraint and operational safety, only air and magnetic bearing forms can be applied to our developed mini-type air turbine cartridge. Without adding any extra power source, the air bearing can directly use the same pressured air source supplied to the air turbine cartridge. The Reynolds equation [1], the differential equation relative to pressure, density, relative velocity and lubrication film thickness, not

only achieved the basic theories of hydromechanics, but also established the basis for the current development of air bearing. But for realizing well-working air bearing, it needs also deliberated design and precision machining processes.

For performing more and more miniature and precision machining tasks, high-speed spindle already becomes a requisite part of advanced precision machines. And the development of frictionless and precision bearings also becomes crucial issue. After long-term studies and developments, high-speed spindles equipped with aerostatic bearings gradually become commercial products. In the developed ultra-precision vertical machining center of Toshiba, they applied aerostatic bearing to achieve spindle speed up to 60 krpm. The Company Westwind [2] also utilized aerostatic bearing to invent a PCB drilling machine with a spindle speed up to 250 krpm. And Uni-Tek System Wu et al. [3] set up a 50 krpm high-speed aerostatic spindle to drive diamond cutter in their wafer cutting machine. As to dental handpieces, NSK has once developed product integrated with aerostatic bearing. Afterward, Fukuyama [4] applied porous material to create aerostatic bearing component, as well as Nakayama and Ogino [5] proposed a patented design for aerostatic bearing. As to basic theoretical and development researches, Mizumoto and Matsubara [6] have experimentally studied the bearing stiffness of axial aerostatic bearings, Yoshimoto [7] has designed the aerostatic bearing sizes of different models of aerostatic bearings by using Reynolds Equation, Noguchi [8] has proposed the influence evaluation of aerostatic bearing on rotation precision; and Fukuyama [4] has clearly forecasted the developing trend of aerostatic bearing, i.e., high speed, high stiffness and high precision. As for hybrid bearing idea, Tan et al [9] have developed a permanent magnetic-hydrodynamic hybrid journal bearing, whose axial bearing support comes from magnetic repulsive force and hydrodynamic film induced by rotating spindle. However, its magnetic radial bearing is only activated during the starting and stopping phases of the rotor.

The size of the air turbine cartridge used in dental handpiece is limited to the maximum outside diameter of 10 mm and the maximum length of 12 mm. Besides spindle, turbine rotor and shell, the bearing can only occupy 1/3 total volume of the air turbine cartridge. The constrained size and small bearing surface on the spindle bring out large challenge to achieve sufficient aerostatic bearing support. Besides, the pressured air used in aerostatic bearing can also easily induce instable operation because of air compressibility. Therefore, we come to an idea to integrate a magnetic levitation into an aerostatic bearing to create a hybrid bearing.

Magnetic levitation can be realized by passive and /or active magnetic devices, which rely on permanent magnet and/or magnetic coil to generate attractive or repulsive forces for non-contact levitation. Because of easy controllability and high power density, diverse magnetic levitations have been developed and widely applied in many advanced precision instruments and machines. For realizing our hybrid bearing in this confined space, only permanent magnet can be adopted to produce repulsive levitation force. Furthermore, repulsively working

permanent magnets can also induce a damping effect while the working gap is decreasing. And this damping effect can just balance the instability induced by aerostatic bearing. But the shape and size of permanent magnet are limited due to its manufacturing and magnetization conditions. In consideration of their characteristics and limitations, the hybrid bearing is analyzed and optimized in order to combine advantages derived from aerostatic and magnetic bearings.

2. DESIGN AND DEVELOPMENT

2.1 Concept

Figure 1 shows the construction of a traditional mini-type air turbine cartridge, which integrates an air turbine, a spindle and two ball bearings into a very confined housing, whose size is limited within the outside diameter of 10 mm and the length of 12 mm. The air turbine is responsible for energy transformation from high pressured air to mechanical rotational energy. The spindle transfers the mechanical energy to the attached machining tool. And the two ball bearings are used to support the spindle for allowing a stable rotation. During the high-speed spindle rotation phase, the balls inside each ball bearing will be intensively agitated by the frictional contact with the bearing ring, thus generating impact vibration and noise to interfere with the spindle rotation and induce thermal loss and serious wear. Although a radial preloading for the ball bearing can improve its radial run-out, the contact friction brings always disturbances for the high-speed operation.

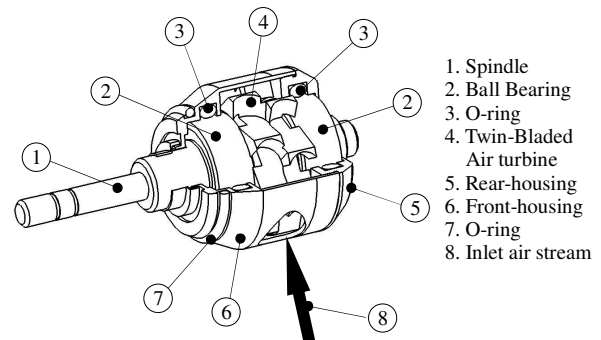


Fig. 1 Traditional mini-type air turbine cartridge

For increasing the speed and stability of the air turbine cartridge, the air turbine and the bearings are the main determined parts. Besides the new design of the air turbine, the development of the non-contact bearing can consequently enhance the air turbine to reach a frictionless and stable rotation, which can thus increase its rotation speed. Because of its limited space and operational condition, only pressured air and permanent magnet can be applied to realize the non-contact bearing without adding any extra power source or complicated device. A pressured air source can be simultaneously used to drive the air turbine and the air bearing. Furthermore, due to the variable operational speed, the aerostatic bearing is more suitable than the aerodynamic bearing to fulfill the non-contact function. In comparison with the requirement of fine and

complicated aerodynamic texture on the bearing surface, the aerostatic bearing only needs a well-machining slick bearing surface with orifices and/or recesses. The main purposes of the orifices are to build up a pressured air film in air gap and to block the air perturbation from the air supply. And the recess around each orifice is responsible to create a homogenous air pressure zone that can significantly increase the bearing stiffness and capacity.

According to the research result as shown in Wang and Huang [10], the air turbine cartridge supported by two ball bearings can reach a speed of 300 krpm by 3 bar air pressure. After applying a patented aerostatic bearing, the air turbine cartridge designed by Sugai and Nakayama [11] can run under a speed of 500 krpm also by 3 bar air pressure. The performance of the aerostatic bearing has been approved that its non-contact operation can enhance the speed of the air turbine cartridge by about 50% or even higher. Normally, the bearing surface of the aerostatic bearing must be hardened and polished to allow dry sliding during the air shortage or vanishing phase. However, the air bearing also possesses some drawbacks induced by the air compressibility. Through the air compressibility, any run-out of the spindle can make the air pressure in a compressed or choked air gap rapidly increase. Furthermore through strongly decreasing air gap, the air flowing velocity increases so drastically that its sinking air pressure acts like a vacuum to force the air gap reduce. But this compressed air gap acts like a spring that can store enough potential energy to react against the spindle run-out. The kinematic relationship between the spindle and the air gap is equivalent to a mass-spring vibration model. A spindle run-out affects two opposite-working air gaps, thus inducing spindle vibration and impact noise. This phenomenon is the pneumatic hammer effect, as shown in Figure 2(a), which severely spoils the stable and precision spindle rotation.

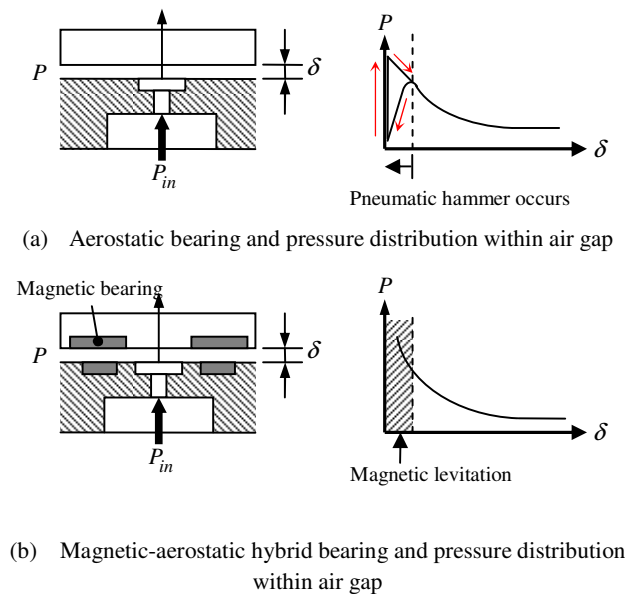


Fig. 2 Schematic concepts and characteristics

The integration of the permanent magnets into the aerostatic bearing is to create a sufficient repulsive force to avoid pneumatic hammer effect, as shown in Figure 2(b). The repulsive magnets can increase the bearing stiffness and capacity of the hybrid bearing, and it can produce some damping effect because of the very close magnetic interaction. For protecting the unavoidable collision, the brittle magnets must be kept away from the high-speed

2.2 Function and Construction

Figure 3 shows the new developed air turbine cartridge with the magnetic-aerostatic hybrid bearing. The air turbine with new designed shape is fixed to the spindle. On the both sides of the air turbine, there is a pair of hybrid bearings symmetrically installed. And each hybrid bearing consists of an aerostatic radial bearing, an aerostatic axial bearing and a magnetic axial bearing. Two repulsively working magnet rings are used to build up each magnetic bearing with a magnet stator and a magnet rotor. Because of form and magnetization limitations of magnet, only the magnetic axial bearing is developed to resist the axial working force. A pair of magnet rotors is fixed on the both sides of the air turbine and rotates together with the spindle. The other pair of magnet stators are well integrated with the aerostatic bearings. The dynamic energy of the high-pressure air is transformed by the air turbine into the mechanical rotational energy for the spindle. Furthermore, the symmetrical form of the turbine blades mainly induces the radial force and creates less axial force on the spindle. Besides the airtight sealing function in the housing, the elastic O-ring also allows the supported bearing part the self-alignment in order to avoid getting stuck. The air-supply channels for the aerostatic bearings are separate from the air inlet for the air turbine, and they are constructed inside the reserved hollow spaces between the housing and the bearing parts.

The two aerostatic radial bearings are installed on the both ends of the spindle in order to produce large enough moment against spindle tilting motion. In addition, the aerostatic axial bearings oppositely direct at the both magnet rotors. Each magnet stator is placed between the aerostatic radial bearing and the aerostatic axial bearing. Through the aerostatic axial bearing, the magnet rotor and the magnet stator are physically separated from each other, but their repulsive magnetic fields can still affect each other.

During the intermittent starting and free rotation phases, the two magnetic bearings symmetrically produce repulsive magnetic forces from both sides to the air turbine to depress run-out vibration. Furthermore, during its working operation, the magnetic bearings will retard the rapid air-gap reduction in the aerostatic axial bearing to avoid inducing air hammer effect. The magnetic bearings work as auxiliary units to enhance the high-speed operation stability for the air turbine cartridge.

Because of the small size of the cartridge, the surface curvature of the spindle is so large that the difficulty for manufacturing the orifices on the aerostatic radial bearing rises. For economically realizing precision orifices, we develop the composite orifice form with a large depth to

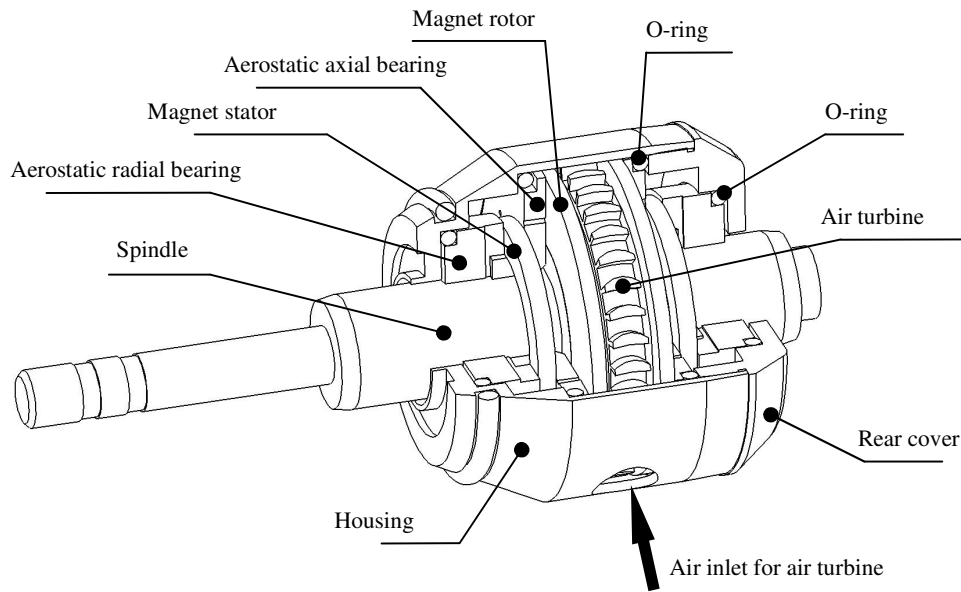


Fig. 3 Construction of new developed air turbine cartridge with magnetic-aerostatic hybrid bearings

width aspect ratio. The composite orifices in the aerostatic radial bearing are built up between two parts; only one part is processed with the orifice notches by using a 0.1mm thin saw blade, and it is covered by the flat side-surface of the axial bearing sleeve. The orifices with a large depth to width aspect ratio can also decrease the air fluctuation and increase the air-film stiffness, thus improving the bearing stability and capacity. Figure 4 shows the composite orifices and the drilling orifices on the aerostatic axial and radial bearings.

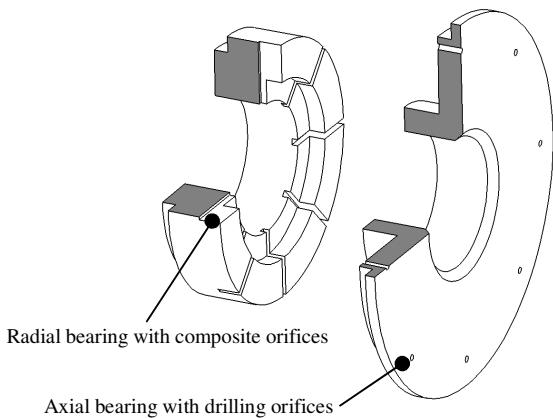


Fig. 4 Composite orifices and drilling orifices on aerostatic bearings

3. ANALYTICAL VERIFICATION

Because of the complicated and compact structure of our developed air turbine cartridge with the hybrid bearing, it is very difficult to derive a reliable and complete physical equation that can describe its whole characteristic function.

Therefore, we must rely on the application of the advanced tools- the finite element analytical (FEA) software ANSYS® and the computational fluid dynamics (CFD) software FLUENT® to detailedly analyze the aerostatic bearings. Figure 5 shows the entire pressure distribution inside the aerostatic axial and radial bearings for the input air-pressure of 3 bar. While the pressure significantly sinks from each orifice to its nearest outlet, the pressure distribution on the zone between the axial and radial orifices is well maintained. However, the bearing gap also influences the pressure distribution. The radial bearing gap is determined by design, manufacture and wear; and in addition to these similar influences, the axial working force also affects the axial bearing gap.

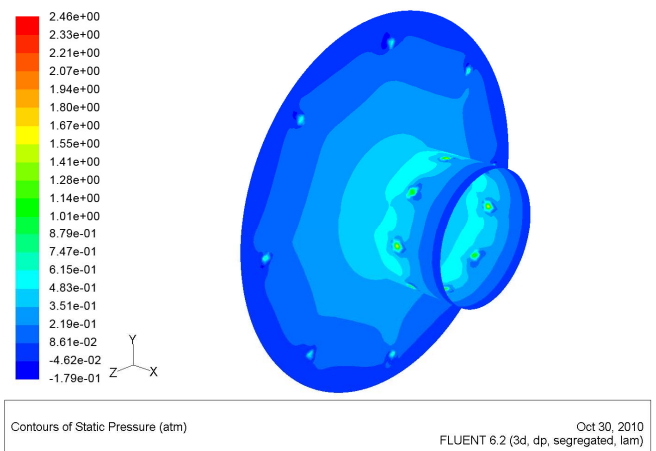


Fig. 5 Entire pressure distribution inside aerostatic axial and radial bearings

3.1 Aerostatic Bearings

Under some standard assumptions :(a) ideal air, (b) fully developed boundary laminar flow, and (c) constant temperature, the relations of the bearing capacities W_a and W_r to the design and operational parameters are displayed in Equation (1) and (2). Through the integration of the pressure distribution on the bearing surface, its corresponding bearing capacity is then derived.

Axial bearing capacity W_a :

$$\frac{w_a}{2\pi RLp_a} = \frac{1}{2\pi} \int_0^{2\pi} P \cos \theta d\theta dZ + \frac{1}{2\pi} \int_0^{2\pi} (\tau_x / p_a) \sin \theta d\theta dZ \quad (1)$$

Radial bearing capacity W_r :

$$\frac{w_r}{2\pi RLp_a} = \frac{1}{2\pi} \int_0^{2\pi} P \sin \theta d\theta dZ + \frac{1}{2\pi} \int_0^{2\pi} (\tau_x / p_a) \cos \theta d\theta dZ \quad (2)$$

where R and L is radius and length of air bearings, p_a is inlet pressure, pressure distribution P on the bearing surface, and shear stress τ_x

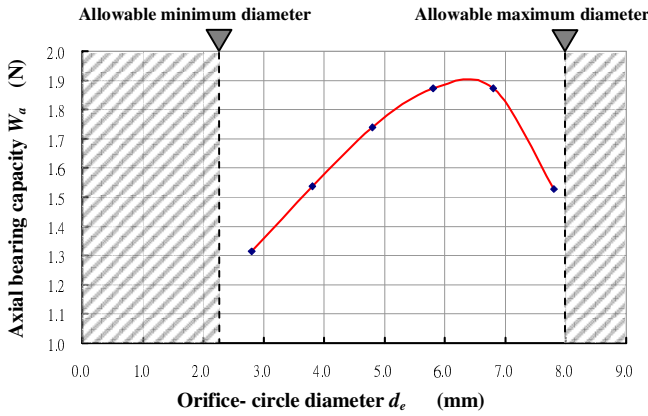


Fig. 6 Influence of orifice-circle diameter on the axial bearing capacity for air pressure of 3 bar

The orifices of the aerostatic axial bearing distribute about an orifice circle, whose diameter d_e also affect its pressure distribution, thus influencing the bearing stiffness and capacity. Figure 6 presents the influence of the orifice-circle diameter d_e on the axial bearing capacity W_a for air pressure of 3 bar. The maximum axial bearing capacity $W_a=1.9$ N occurs around the diameter $d_e \approx 6.5$ mm. For the orifice-circle diameter up to 6.5 mm, the larger the orifice-circle diameter, the larger bearing surface around the spindle center to build up bearing pressure, also resulting in higher bearing capacity. However, once the orifice-circle diameter d_e is more than 6.5 mm, the bearing capacity obviously decreases, since orifices distribute much nearer to the exhaust margin, from which the high-pressure air easily leaks, thus causing loss of pressure and bearing capacity.

$$\eta_B = \frac{P_{op}}{P_{in}} \quad (3)$$

The other significant criterion for bearing is the bearing efficiency η_B , which is the ratio the bearing operating power P_{op} to the input power P_{in} . While the input power comes from the product of the supplied air pressure P and volume-flow rate Q_{in} , the bearing operating power is the output power for supporting the spindle rotation. The higher bearing efficiency, the less operation loss induced in the bearing. If the change of air density does not be considered, the influence of the orifice-circle diameter on the axial bearing efficiency can be derived as shown in Fig. 7. The position of the maximum bearing efficiency widely spans around the orifice-circle diameter of 5-7 mm, and it overlaps with that of the maximum bearing capacity. Besides, the maximum bearing efficiency can also exceed 95%.

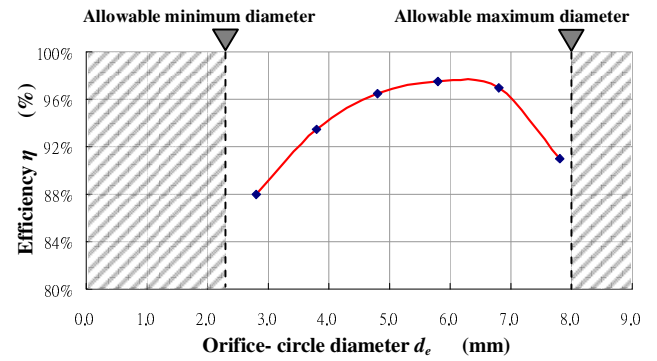


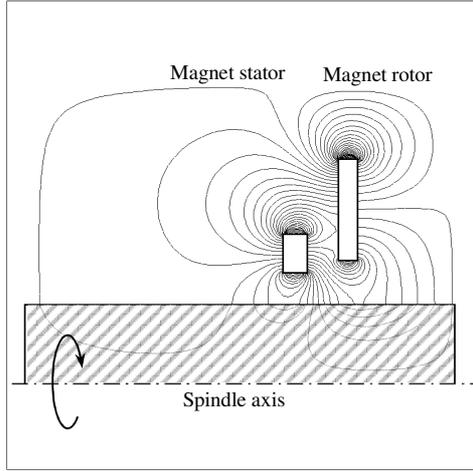
Fig. 7 Influence of orifice-circle diameter on the axial bearing efficiency for air pressure of 3 bar

3.2 Magnetic Bearing

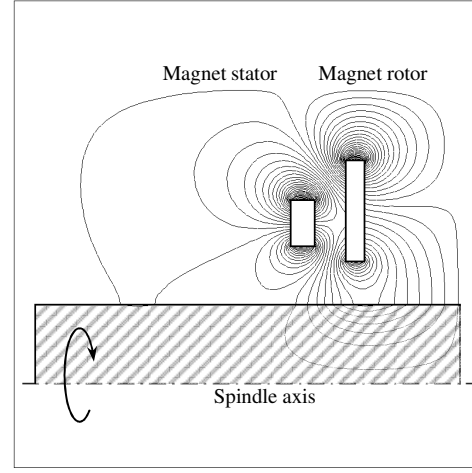
Due to the space limitation and the orifices of the aerostatic axial bearing, the size of the magnet stator must be smaller than the magnet rotor. These magnet rings are made of sintered NdFeB-N45SH magnet, whose magnetic characteristics are: $B_r=13.2$ kGs, $H_c=20$ kOe, and $(BH)_{max}=45$ MGOe. For realizing efficient magnetic analysis, the FEA-software ANSYS and the simplified 2D-axisymmetric module are applied for the magnet rings. Figure 8 shows the magnetic flux distributions induced by two developed configurations with magnet stator and magnet rotor. In the radial-offsetted configuration, the magnet stator is radial-offsetted to the magnet rotor. Because the outside margin of the magnet stator is very close to the inner hole of the magnet rotor, their fluxes are linked together and acts as attraction instead of repulsion. In the radial-symmetrical configuration, the magnet stator directly faces toward the magnet rotor. According to the magnetic opposite-acting flux interactions, the radial-symmetrical configuration can realize stronger repulsive effect. Their repulsive forces F_1 and F_2 between the magnet stator and the magnet rotor are described as follows

$$F_2 = -F_1 = -\frac{\mu_0 \bar{j}_1 \bar{j}_2}{4\pi} \iint \iint \frac{\bar{r}(ds_1 ds_2)}{|\bar{r}|^3} \quad (4)$$

where is μ_0 permeability of air, \bar{r} is the location vector between the magnet stator and the magnet rotor, and \bar{j} is the magnet vector



(a) Radial-offsetted configuration



(b) Radial-symmetrical configuration

Fig. 8 Magnetic flux distributions for two developed configurations with magnet stator and magnet rotor

Figure 9 is the magnetic field-density distribution of the radial-symmetrical configuration. Its field intensity concentrates on the inner holes and outside margins of magnet rings. Through integration over the side-surface of the magnet rotor, the axial bearing capacity- the repulsive force- of 1.43 N is derived.

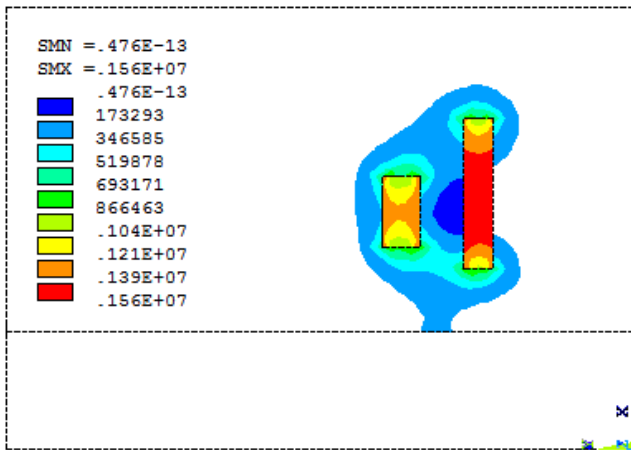


Fig. 9 Field intensity distribution of radial-symmetrical configuration

3.3 Dynamic Performance

For realizing high-speed performance, the air turbine is made of light-weight aluminum alloy, and the spindle needs a large strength and is made of stainless steel.

According to the equation derived by Dyson and Darvell [12] as shown in Eq. (6), the free running speed \hat{N}_f of the air turbine cartridge with ball bearings is influenced by the temperature T , the inlet air pressure P_{og} , the radius of the air turbine r and the pressure effectiveness of the air turbine α . In addition, the pressure effectiveness α is equivalent to the Mach number on the turbine tip.

$$\hat{N}_f = 5.0358 \frac{\sqrt{T}}{r} \cdot \sqrt{1 - (1 + \alpha P_{og})^{-0.2867}} \quad (6)$$

By a temperature $T = 303^\circ \text{K}$ and the conditions of the air turbine cartridge: $r = 4.45 \text{mm}$, $\alpha = 0.288$ and $P_{og} = 3 \text{bar}$, the air turbine supported by ball bearings can theoretically achieve the free running speed of 478 krpm. Moreover, the application of the frictionless magnetic-aerostatic hybrid bearings can significantly enhanced its free running speed.

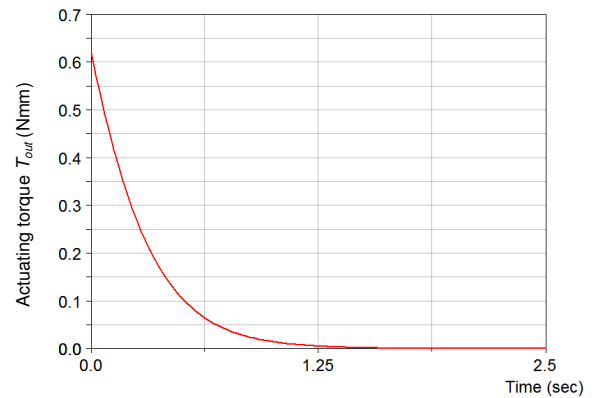


Fig 10 Actuating torque during starting phase

For comprehending its dynamic performance, the multibody dynamics software ADAMS[®] is utilized to analyze the actuating torque and the speed. In addition, for conforming with actual physical condition, the simulation also takes the influences from air resistance, outlet pressure, inlet air momentum, rotational inertia, and air film resonance in consideration. By supplying 3-bar air pressure, the air-flow rate Q_{in} for the air turbine cartridge is about 15 l/min. Therefore, through the air blowing energy on the turbine blade, the tangential acting force and its actuating torque T_{out} can be analyzed. Figure 10 describes the actuating torque T_{out} during a starting phase. At the first air blowing moment, the actuating torque T_{out} reaches its

maximum of 0.62 Nmm. As the rotation speed of the turbine rapidly increases, the actuating torque simultaneously sinks. In addition, Figure 11 shows its corresponding starting process for the rotation speed N_r . The starting phase approximates 0.6 s, which is the rising time to reach about 63% the maximum free running speed of 500 krpm.

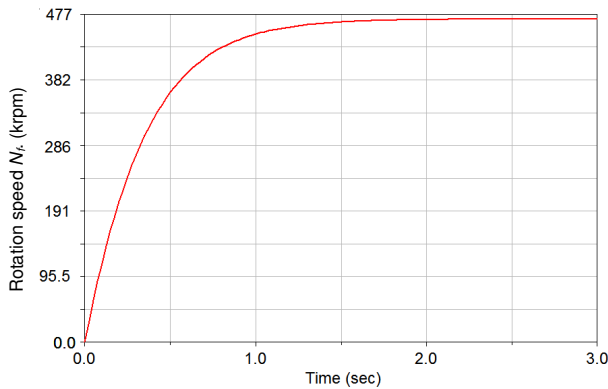


Fig 11 Starting process for rotation speed

In our developed hybrid bearing, the magnetic bearings are designed for enhancing bearing stability and capacity of the aerostatic bearing. Our analyses are focused on the instant response and the axial swaying stability. Figure 12 shows the dynamic reactions of the aerostatic bearing and the hybrid bearing after an interference of axial force impulse, which can easily induce pneumatic hammer effect for the aerostatic bearing. Its vibration decays gradually, and after 5 swings the amplitude comes to 15% of the initial value. However, the repulsive magnetic levitation in the magnetic-aerostatic hybrid bearing can effectively damp the pneumatic hammer vibration and also slows down the instant reaction.

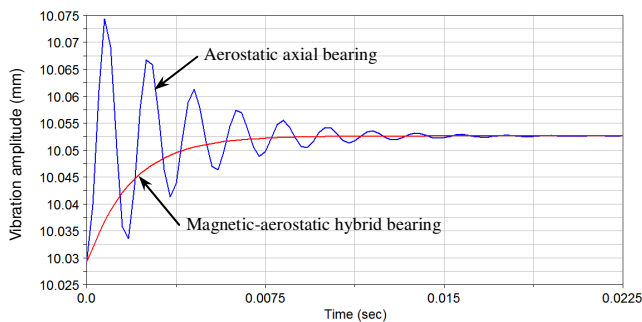


Fig. 12 Dynamic reactions of aerostatic bearing and hybrid bearing after an interference of axial force impulse

During the free running phase without any external interference, tiny unavoidable unbalance inside the rotating rotor, air turbulence and magnetic field inhomogeneity will cause the high-speed spindle sway. In addition, the air film elasticity also promotes the axial swaying vibration. Figure 13 indicates that the axial swaying vibrations of the rotating spindle supported by the aerostatic bearing and the hybrid bearing. The magnetic levitation has significant effect to depress the axial swaying vibration. Moreover, reducing the vibration amplitude from 0.015mm to about 0.006mm can

effectively improve the stability and rotation precision of the rotating spindle.

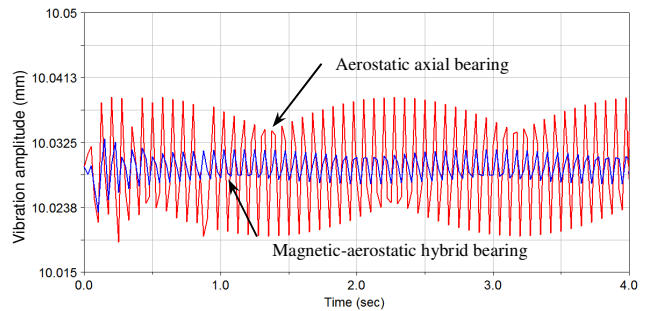


Fig. 13 Axial swaying vibrations of rotating spindle supported by aerostatic bearing and hybrid bearing

4. CONCLUSION

For enhancing speed and durability and to decrease noise and vibration in high-speed operation, a novel non-contact hybrid bearing is designed and developed for an air turbine cartridge built in the dental handpiece. And the hybrid bearing integrates the magnetic axial bearing into the aerostatic axial bearing. By using the same air supply for the air turbine, the aerostatic bearing can provide a frictionless and vibrationless support for the high-speed spindle. However, the aerostatic bearing has also drawback such as pneumatic hammer effect because of air compressibility. Through unavoidable spindle's run-out induced by external force interference or unbalance, the air gap is so rapidly change that the air film can store potential energy to excite the pneumatic hammer effect. The magnetic bearings are integrated to create a repulsive preload for increasing bearing stiffness and capacity, thus retarding the rapid air-gap reduction and enhancing high-speed spindle stability.

For economically realizing precision orifices, we develop the composite orifice form with a large depth to width aspect ratio. Moreover, the composite orifices can decrease the air fluctuation and increase the air-film stiffness, thus improving the bearing stability and capacity. In order to optimize the bearing capacity and efficiency, the finite element analytical (FEA) software and the computational fluid dynamics (CFD) software have been utilized to analyze the orifice layout of the aerostatic bearing. The magnetic axial bearings with repulsive NdFeB permanent magnets are skillfully built up inside the constrained space of the air turbine cartridge, and its magnetic flux and intensity distributions are analyzed by the FEA-software and the simplified 2D-axisymmetric module. Finally, through the multibody dynamics simulations, they can approve the effect of the magnetic bearing used for the aerostatic bearing. The magnetic bearing can efficiently depress the pneumatic hammer effect and 60 % of the swaying vibration.

REFERENCE

- [1] Reynolds, O., 1886, "On the Theory of Lubrication and Its Application to Mr. Beauchamp Tower's Experiments,

- Including an Experimental Determination of the Viscosity of Olive Oil” , *Philosophical Trans. R. Soc. London*, Vol. 177, pp.157-234.
- [2] Westwind Company website, Available at: www.westwind-airbearings.com, Accessed 1st December 2010.
- [3] Wu, Kuo-Hwa, Chien, Chi-Chien, Chen, Shu-Wen, Seng, Wei-Chun, and Chen, Chun-Chen, 2002, “Device for cutting interconnected rectangular plate-shaped workpieces into a plurality or individual rectangular units” , *U.S. Patent No.6371102*
- [4] Fukuyama H., 1976, “Porous, static pressure air bearing device in a dentist’ s handpiece” , *U.S. Patent No.3969822*
- [5] Nakayama S. and Ogino S., 1985, ” Air bearing device in dental handpiece” , *U.S. Patent No.4521190*
- [6] Mizumoto, H. and Matsubara, T., 1989, “Aerostatically controlled restrictor for obtaining an infinite stiffness aerostatic thrust bearing” , *Bulletin of the Japan Society of Precision Engineering*, Vol. 23, pp.211-216.
- [7] Yoshimoto, S., 2002, “Theory and Operating Principle of Aerostatic Bearings” , *Design Engineering*, Vol. 37, pp.51-56.
- [8] Noguchi, S., 2002, “the influence evaluation of aerostatic bearing on rotation precision” *Design Engineering*, Vol. 37, pp.57-62
- [9] Tan, Q. C., Li, W., and Liu, B., 2002, “Investigations on a permanent magnetic-hydrodynamic hybrid journal bearing” , *Tribology International*, Vol. 35, pp. 443-448.
- [10] Wang, Shih-Chun and Huang, Kuang-Yuh, 2009, “Research and Development of Minitype Twin-Bladed Air Turbine” , *Proceedings of ASME Turbo Expo 2009, ASME International Gas Turbine Institute*, Orlando, Florida, USA, GT-2009-59702, June 8-12, pp. 175-181.
- [11] Sugai, Hiroshi and Nakayama, Shoji, 1980, “Air bearing for a dental handpiece” , *U.S. Patent No.4209293*
- [12] Dyson, J. E. and Darvell, B. W., 1999, “Flow and free running speed characterization of dental air turbine handpieces” , *J. Dent.*, Vol. 27(2), pp.465 – 477.